Hindawi
Advances in Materials Science and Engineering
Volume 2019, Article ID 4592847, 13 pages
https://doi.org/10.1155/2019/4592847

Research Article

Seismic Fragility Analysis of Buildings Based on Double-Parameter Damage Models considering Soil-Structure Interaction

Panpan Zhai,[1,2] Peng Zhao,[2,3] Yang Lu,[2,3] Chenying Ye,[2,3] and Feng Xiong[2,3]

[1]*Institute of New Energy and Low-carbon Technology, Sichuan University, Chengdu 610065, China*
[2]*MOE Key Laboratory of Deep Underground Science and Engineering, School of Architecture and Environment, Sichuan University, Chengdu 610065, China*
[3]*College of Architecture & Environment, Sichuan University, Chengdu 610065, China*

Correspondence should be addressed to Feng Xiong; fxiong@scu.edu.cn

Received 7 June 2019; Accepted 20 September 2019; Published 24 October 2019

Academic Editor: Paweł Kłosowski

Most conventional seismic fragility analyses of RC buildings usually ignore or greatly simplify the soil-structure interaction (SSI), and the maximum interstory drift ratio (MIDR) is often adopted to establish seismic fragility curves. In this work, an eight-story RC building was designed to study the influence of the SSI on the seismic fragility of RC buildings. Three double-parameter damage models (DPDMs) were considered for the fragility assessment: the Park–Ang model, the Niu model, and the Lu–Wang model. Results show that considering SSI induces a higher fragility than that of the fixed model and that employing the DPDMs for the fragility analysis provides more reasonable results than those evaluated using the MIDR damage index.

1. Introduction

Seismic fragility analysis of structures is the basis of seismic loss estimation and city risk management. This type of analysis is helpful in understanding the response of structures under an earthquake so as to define the structural damage corresponding to a specific earthquake intensity level. Therefore, decision-makers can adopt the fragility analysis as a significant reference to reduce the consequences of earthquakes [1].

Developing fragility curves is useful for seismic fragility assessment of structures. In principle, fragility curves can be established using the following methods [2]: (1) professional expert judgement; (2) quasistatic and design code consistent analysis; (3) statistical analysis of damage data associated with past earthquakes; and (4) numerical simulation based on the structural dynamic analysis. Due to the scarcity and low reliability of postearthquake data, the numerical method is the most commonly adopted method in current research.

It is of great importance to include soil in the numerical model in the fragility analysis. When an earthquake appears, the propagation of seismic waves in the soil results in soil movement and is proven that soil-structure interaction (SSI) affects the dynamic responses of the structure. For example, Myat [3] studied the seismic performance of low-rise shear wall buildings with a strip foundation, and the results showed that both the axial forces and shear forces of the columns increased compared with those with the fixed base. Dutta et al. [4] found that the SSI could increase the base shear of a low-rise RC frame building but decreased the seismic response of high-rise buildings. Pinto and Ciampoli [5] investigated typical piers and assessed the effect of SSI on dynamic response, which indicated that in most cases, SSI led to a higher displacement demands than fixed-base structures.

Unfortunately, most existing numerical studies of fragility do not consider the SSI effects and simply fix the bottom of the structure. Only a few works currently include the SSI effects in the structural fragility analysis, which shows

the changes caused by the SSI effect. For example, the study of Rajeev and Tesfamariam [6] highlighted the effects of the SSI on three-, five-, and nine-story, three-bay moment reinforced concrete frames resting on dense silty sand, and the fragility curves were developed for both fixed-base and SSI models. The results showed that the SSI effect induced higher fragility than that of the fixed-base model. Similarly, Pitilakis et al. [7] studied three RC buildings resting on very soft soil, and the comparative fragility curves were obtained with the fixed-base and SSI models. A substantial increase in the fragility was observed for the SSI models with respect to the fixed-base structures. The research of Saez et al. [8] also studied the effects of the SSI on the fragility assessment for an old RC building resting on a mixture of sandy and clayey soil, and a general reduction in the fragility was presented. As is well known, the SSI has a very complex influence on the structural responses; therefore, it does not always lead to beneficial effects. As a result, it is appropriate to study the SSI effects on the structural fragility, which is helpful to generate more accurate fragility curves.

Furthermore, all the seismic fragility analyses above adopt a simplified soil model represented by a series of springs. The characteristics of the springs will influence the structural fragility results. With the development of computing technologies, it is possible to employ a full soil-structure model in the fragility analysis to obtain satisfactory results. On the other hand, the current fragility analysis uses the maximum interstory drift ratio (MIDR) to assess the damage state of structures. The MIDR is the most commonly used metric, as it is easily obtained in the performance analysis of the structure under an earthquake. However, this response parameter cannot fully reflect the cumulative damage caused by the low cycle fatigue under the reciprocating load of an earthquake [9]. Therefore, using MIDR may underestimate the degree of damage, especially when under a long-lasting earthquake, which will lead to severe seismic loss. Because the double-parameter damage models (DPDMs), generally using the combination of deformation and energy as the damage index, can reflect both the maximum deformation and cumulative damage effects, it is considered to be more comprehensive when describing the structural damage under earthquakes, which may give an accurate prediction of the seismic damage of buildings.

In this study, to investigate the SSI effects on fragility assessment and supply a method for the fragility analysis of SSI structures, an eight-story RC frame structure was designed and fully modeled as a test bed to carry out a series of numerical fragility analyses. At the same time, three DPDMs of Park–Ang, Niu, and Lu–Wang model are adopted to evaluate the seismic fragility of structures compared to using the MIDR.

2. Damage Models

The seismic damage model is an important tool to describe the degree of damage to structures under an earthquake, making it a key issue in fragility analyses. In general, the damage model is a quantitative mathematical model describing the severity of damage, measured by a damage index (DI). Through comparing the damage index with the limit values defined for specific damage states, the damage of structures can be assessed. Three typical DPDMs are selected in this investigation, including the Park–Ang model, which is widely accepted in the earthquake engineering field, the Niu model, of which the relevant parameters are easy to determine, and the Lu–Wang model. The expressions of the DPDMs adopted can be seen in Table 1.

In Table 1, δ_m is the maximum displacement under an earthquake, δ_u is the ultimate displacement under a monotonic loading, δ_y is the yield displacement, F_y is the calculated yield strength, E_u is the limit hysteretic energy, E_h is the cumulative hysteretic energy, and β_o is a nonnegative parameter. In the Niu damage model, $\mu = 0.1387$ and $\gamma = 0.0814$. When evaluating the damage that appears in a specified story level or an entire structure, a weighted combining index is required:

$$\mathrm{DI} = \sum_{i=1}^{n} \lambda_i D_i. \tag{1}$$

Some researchers [15–17] proposed different methods to calculate the weighting coefficients. In this study, the method proposed by Du and Ou is first adopted to generate the story level damage index, and the method proposed by Ou and He is then adopted to define the damage index of the total structure. The weighting coefficient method adopted in this study can be seen in Table 2.

To obtain the structural fragility curves, the relationship between the structural response and damage states must be clearly defined. Based on the existing methods, five damage states and four limit states (LS) of slight damage, moderate damage, severe damage, and complete damage are defined, and the corresponding indices of four limit states are shown in Table 3.

3. Numerical Modeling

To study the SSI effects on structural fragility using the DPDMs, a typical eight-story, three-bay reinforced concrete frame building is designed according to the Chinese code for Seismic Design of Buildings [19]. Two foundation systems are considered in this study: fixed-base and piled raft supported on soft soil considering the SSI effects. The dimensions of the reference structure are shown in Figures 1 and 2.

3.1. Superstructure Model. The reference structure adopted in this study is a high-rise building with 8 stories, with a story height of 3.0 m. The building has a floor plan of 6.0 m by 14.4 m with three bays in the horizontal direction (shown in Figures 1 and 2). The section size of the beam is 300 mm by 600 mm and of the column is 800 mm by 800 mm, and the thickness of the floor is 120 mm. The structure is designed using the PKPM software according to the "Code for Seismic Design of Buildings" (GB50011-2010) [18] and the "Code for Concrete Structure Design" (GB50010-2010) [20]. The concrete grade of the beam, column, and floor is C30, and the equivalent elastic modulus is 32000 MPa. The C30

Table 1: The DPDMs adopted in this study.

Damage models	Expression
Park–Ang [10, 11]	$\mathrm{DI} = (\delta_m/\delta_u) + \beta_o(E_h/F_y\delta_u)$
Niu [12]	$\mathrm{DI} = (\delta_m/\delta_u) + \mu(E_h/E_u)^{\gamma}$
Lu–Wang [13, 14]	$\mathrm{DI} = (1-\beta_o)(\delta_m-\delta_y)/(\delta_u-\delta_y) + \beta_o(E_h/F_y(\delta_u-\delta_y))$

Table 2: Weighting coefficient method adopted in this study.

Weighting coefficient	Expression
Du method [15]	$\lambda_i = D_i/\sum D_i$
Ou method [16]	$\lambda_i = (N+1-i)/\sum_{j-1}^{N}(N+1-j)$

Note: D_i = weighting coefficient for component i or story i; λ_i = damage index of component i or story i; N = the number of stories.

concrete and HRB400 rebars (with a reinforcement ratio of 0.1%) were used, and the reinforced concrete was treated as a bulk material that has been shown to give reasonably accurate results [21–23]. The multilinear isotropic strengthening (MISO) constitutive model in ANSYS was used to simulate the material behaviour. The MISO model was calibrated against Pan's [24] uniaxial compressive stress-strain curves.

To analyse the structural responses, the ANSYS software is employed. The structure and the soil are meshed as in Figure 3. In the model, the floor of the structure is simulated using the Shell181 element, and the beams, columns, and piles are all simulated using the Beam188 element.

In addition, the weight of superstructure and soil is added to the calculation model by means of concentrated nodal force, in which the live load of the floor and the weight of the wall in the frame design is considered, to balance the computational efficiency. The live load of the floor and the weight of the walls are all loaded on the floor, and the mean value of 9.2 kN/m^2. Due to the large scale of the SSI system, the finite element model consists of a total 137,216 elements.

3.2. Soil Model. When considering the SSI in the fragility analysis, it is crucial to determine the range of the soil to ensure the reliability of the analysis. Because the proper size of the soil has a considerable influence on the results of the numerical analysis, Lu and Jiang [25] studied the soil domain range using the displacement response analysis method. The results showed that the soil domain should be taken as at least 8L (L is the width of the structure) with more than 10L yielding very satisfactory results.

Therefore, the size of the soil is defined to be 180 m by 180 m (more than 10L), and the depth of the soil is 20.0 m. The Drucker–Prager constitutive model can better reflect the soil characteristic when simulating the soil elastic-plastic constitutive relation, and the model requires several parameters consisting of the elastic modulus, the Poisson ratio, the density, the soil cohesion, and the internal friction angle. In addition, the Drucker–Prager model has achieved good results in soil constitutive simulation through many practical engineering verifications; therefore, it is adopted in this study [26, 27]. An average shear wave velocity of $V_{s,30}$ equal to about 200 m/s is used, corresponding to ground type II of the Chinese code for seismic design of buildings. A very soft soil is specifically selected to amplify the effects of SSI. The damping ratio for energy dissipation during seismic loading is equal to 5%. The specific soil parameters can be seen in Table 4.

The soil is modeled using the Solid185 element. To simulate the contact performance in the interface between the soil and the pile, the contact elements are employed in this study, where the target surface used the Target170 element and the contact surface used the Contact173 element.

3.3. Input Ground Motions. A representative series of earthquake ground motions are selected for the dynamic analysis, including 5 real ground motion recordings (Table 5) selected from the Ground Motion Database of the Pacific Earthquake Engineering Research Center (*PEER*: http://peer.berkeley.edu/) according to the target spectrum of the Chinese codes. The earthquake magnitudes are $5 < M_w < 8$, and the epicentral distances are $0 < R < 25$ km. Because the foundation soil used in the study, on average, belongs to the soil category according to GB50011, with a $V_{s,30}$ lower than 500 m/s, the selected ground motions were all recoded on soil sites with $V_{s,30}$ ranging from 288 to 413 m/s. Figure 4 shows the spectra of these five ground motions. The soil-structure interaction system is first analysed under the self-weight loading to achieve a geostatic condition, and then the selected ground acceleration time series are applied to the bottom of the soil layer.

4. Dynamic Analysis

To illustrate the effect of different intensities of seismic ground motions on the structural damage distribution using the DPDMs of Park–Ang, Niu, and Lu–Wang compared with that using MIDR for the analysed building with or without SSI effects, a series of preliminary comparative dynamic analyses are conducted for the SSI and fixed-based models based on Park–Ang, Niu, and Lu–Wang damage models with respect to the MIDR under different intensities of seismic ground motions. The TaiwanSMART1(5) earthquake record is used in this case as the input motion, scaled to reach PGA values of 0.1 g, 0.2 g and 0.4 g.

Figures 5–7 show the heightwise distribution of MIDR and the story DI based on the DPDMs of Park–Ang, Niu, and Lu–Wang at different seismic intensity levels of 0.1 g, 0.2 g and 0.4 g, respectively. It can be seen that the SSI effects lead to higher MIDR compared with the fixed-base model. The MIDR of the building considering SSI effects is concentrated at the first story, but the MIDR of the fixed-base building appears at the third story. For the damage distribution of the building using the DPDMs, it is shown that the maximum damage appears at the second story for the fixed-base building and that at the first floor for the building considering SSI effects. The results show that SSI effects will influence the damage distribution of the structure using both

Table 3: Damage indices of the limit state.

Limit state	Slight damage	Moderate damage	Extensive damage	Complete damage
MIDR [18]	1/450	1/300	1/150	1/50
Park–Ang [10]	0.1	0.25	0.4	1.0
Niu [12]	0.2	0.4	0.65	0.9
Lu–Wang [13]	0.2	0.4	0.6	0.9

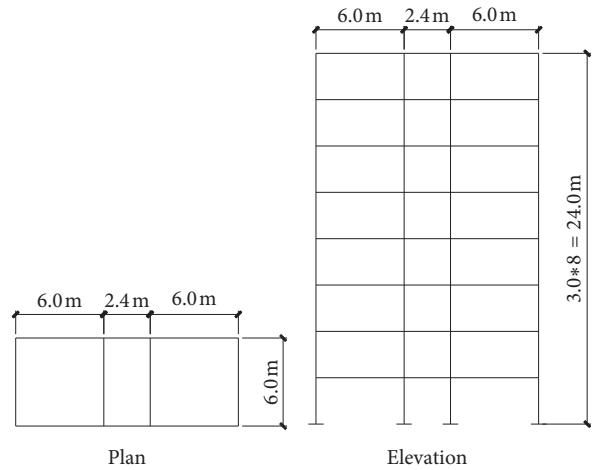

Figure 1: Dimensions of the fixed-base model.

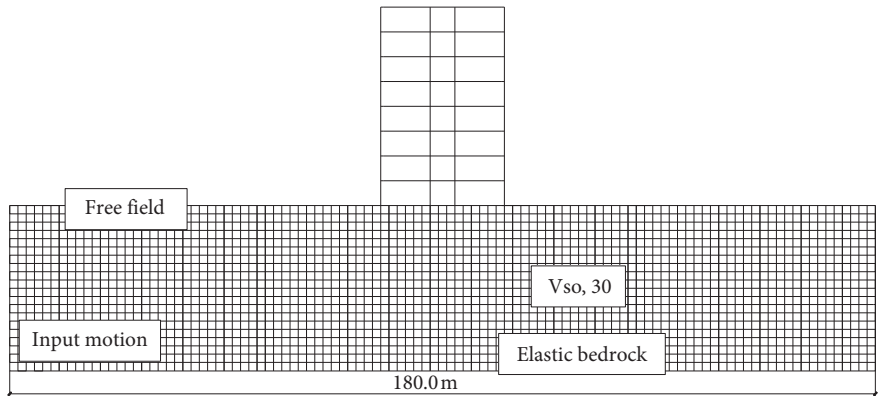

Figure 2: Dimensions of the SSI model.

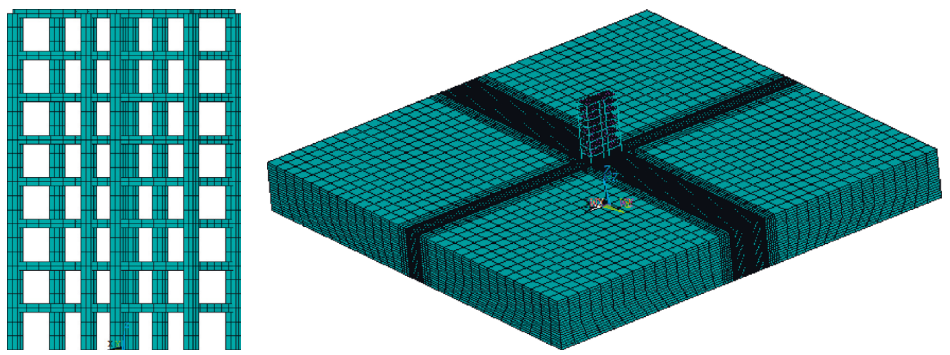

Figure 3: Three-dimensional finite element meshes of the structure adopted in this study. (a) Fixed-base model and (b) SSI model.

Table 4: Parameters of soil.

Thickness (m)	Density (kg/m^3)	Shear wave velocity (m/s)	Passion's ratio	Damping ratio	Shear modulus (MPa)	Elastic modulus (MPa)	Cohesion (Pa)	Internal friction angle (°)
5	2000	190	0.4	0.05	20	48	25000	15
5	2100	200	0.4	0.05	20.4	72.58	40000	20
10	2200	210	0.4	0.05	43.12	103.49	50000	25

Table 5: List of earthquake records used for analysis.

Earthquake recording	Station	Year	M_w	R (km)	PGA (g)	$V_{s,30}$ (m/s)
Parkfield	Cholame-ShandonArray #5	1966	6.19	9.5	0.391	289
Ma.Nicaragua-01	Managua, ESSO	1972	6.24	4.06	0.26	288
Friuli, Italy-02	Forgaria Cornino	1976	5.91	14.75	0.225	413
San Fernando	LA-Hollywood Stor FF	1971	6.61	22.27	0.225	316
TaiwanSMART1(5)	SMART1 007	1981	5.9	24.93	0.085	314

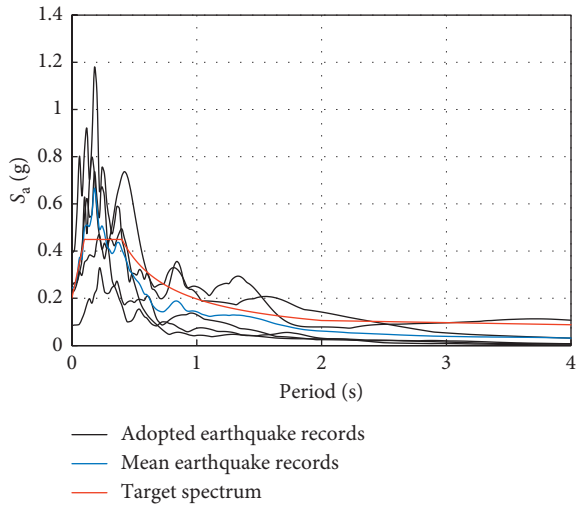

Figure 4: Response spectra of the selected input seismic ground motions.

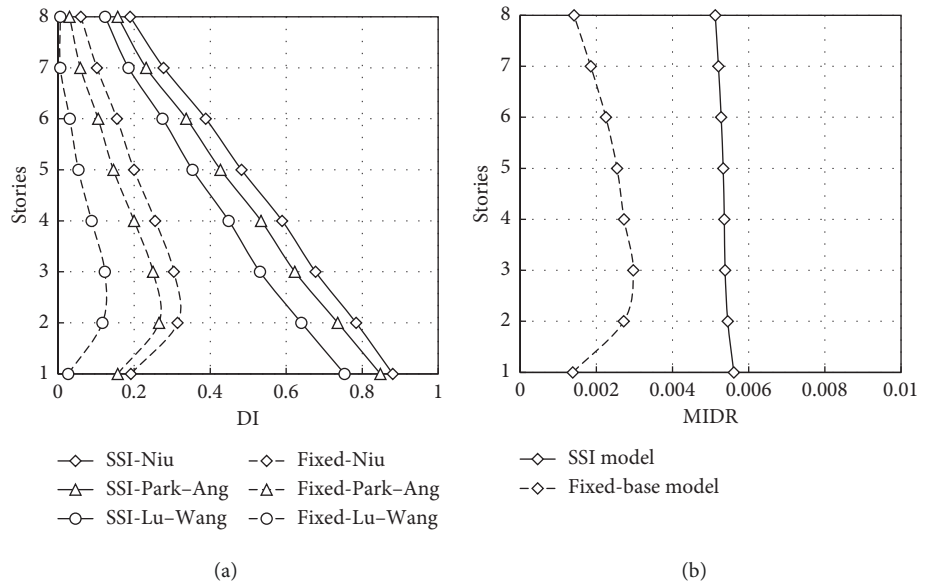

Figure 5: Distribution of damage at PGA of 0.1 g with DPDMs (a) and the MIDR (b).

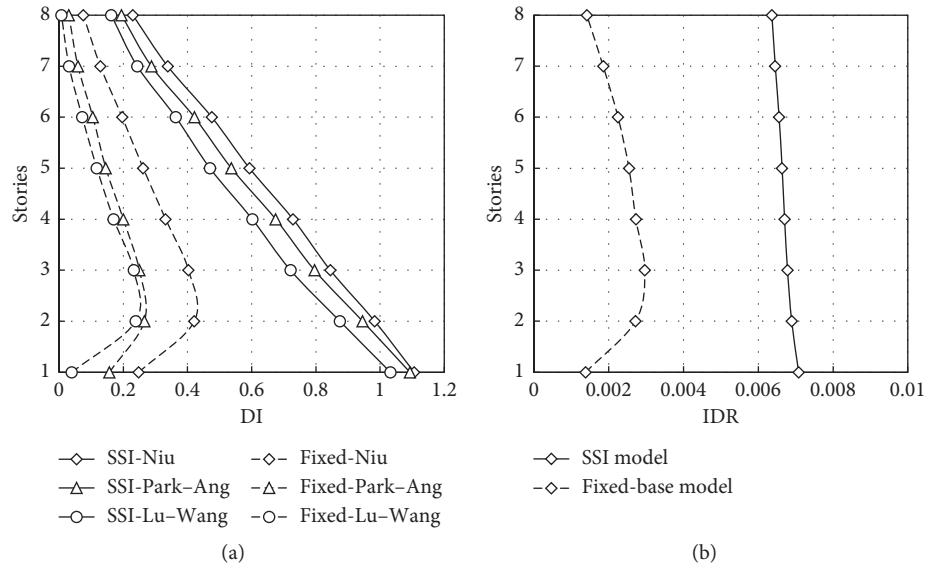

Figure 6: Distribution of damage at PGA of 0.2 g with DPDMs (a) and the MIDR (b).

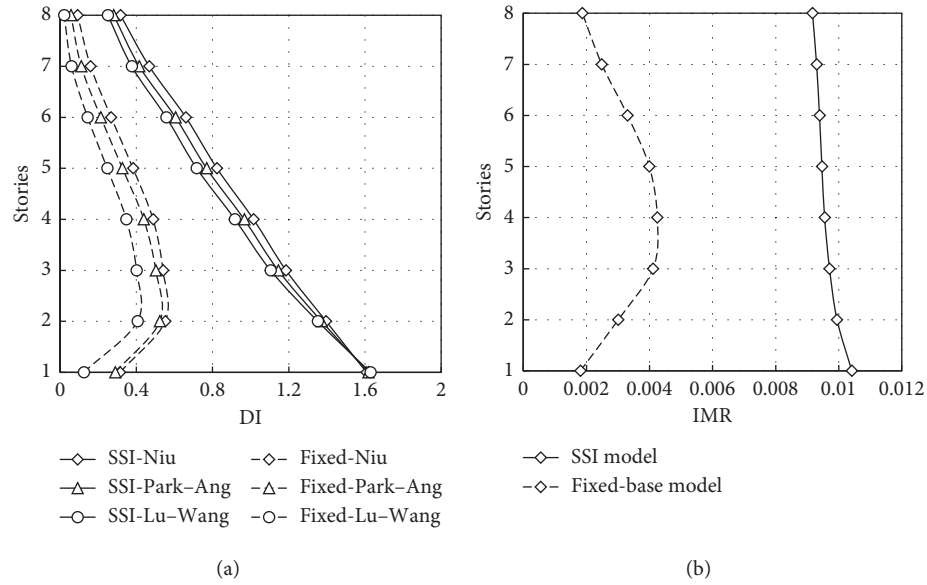

Figure 7: Distribution of damage at PGA of 0.4 g with DPDMs (a) and the MIDR (b).

the DPDMs and the IMDR. In addition, the maximum damage of the fixed-base model is concentrated at the second story using the DPDMs, and the MIDR appears at the third story, but the maximum damage is concentrated at the first floor using the DPDMs and the IMDR for the building considering SSI effects. It is shown that the influence of the damage distribution of the SSI model using the DPDMs compared with the IMDR is different from that of the fixed-base model. The corresponding influence of SSI effects and the difference using the DPDMs and the MIDR is similar under different intensity levels of seismic ground motions.

Figure 8 gives the global DI of the structure under different ground motions of the three DPDMs and the MIDR. It depicts that SSI effects induce higher DI for both the DPDMs and the IMDR. For the building considering the SSI effects, it can be seen that when the PGA is 0.4 g, the structure assessed using DPDMs is in complete damage state, while that evaluated using MIDR is in the severe damage state, showing a large difference of results using different DI. In addition, with the increase in PGA, the difference in damage assessment using DPDMs is more noticeable than the MIDR.

5. Seismic Fragility Analysis

5.1. Incremental Dynamic Analysis. The Incremental dynamic analysis (IDA) is an effective analysis method that involves performing a series of nonlinear dynamic analyses

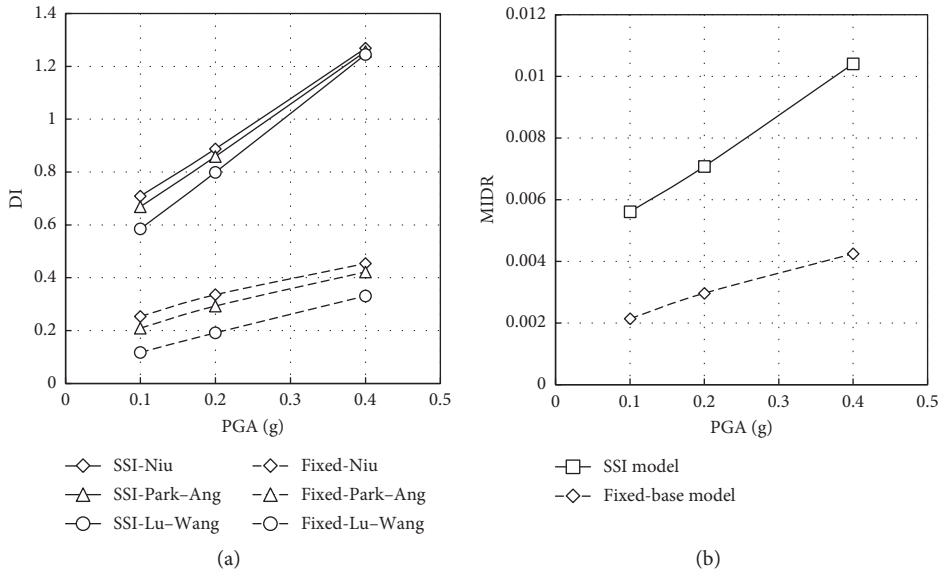

Figure 8: Distribution of the global damage index under different intensities of seismic ground motions with DPDMs (a) and the MIDR (b).

under a suite of scaled ground motion records whose intensities should ideally cover the entire range from elasticity to the whole dynamic instability [28]. An advanced tracing algorithm of Hunt and Fill is used to scale the earthquake records. The PGA is adopted as the intensity measure (I) for the IDA analysis, and each earthquake record is scaled for 10 different levels (i.e., 0.05 g, 0.15 g, 0.225 g, 0.3 g, 0.4 g, 0.5 g, 0.625 g, 0.75 g, 0.8 g, and 0.85 g). Based on the dynamic analyses above, for both the fixed-base models and SSI models, the uncertainty of the input seismic motions, and 50 typical structural samples are obtained for fixed-base model and the SSI model to conduct the fragility analysis, respectively.

5.2. Fragility Analysis. Seismic fragility refers to the failure probability under different seismic intensities, which also describes the seismic performance of the engineering structures in the sense of a probability. Seismic fragility expresses the relationships between the damage degree and the seismic intensity macroscopically using fragility curves. The response results of the IDA are used to derive fragility curves expressed as double-parameter lognormal distribution functions. The cumulative probability of exceeding an LS conditioned on a measured of the seismic intensity IM is as follows [29]:

$$P_f(\mathrm{LS} \mid \mathrm{IM}) = \Phi\left\{\frac{\ln(\mathrm{IM}) - \ln(\overline{\mathrm{IM}})}{\beta}\right\}, \quad (2)$$

where Φ is the standard normal cumulative distribution function, IM is the intensity measure of the adopted earthquake expressed in terms of PGA (in units of g), $\overline{\mathrm{IM}}$ and β are the median values (in units of g) and the log-standard deviations of the building fragilities, and LS is the limit state. The median PGA values corresponding to the prescribed performance levels are determined based on a regression analysis of the nonlinear IDA results for each structural model. Figure 9 illustrates the PGA-MIDR relationships and PGA with double-parameter damage index for the fixed-base structural model and the structural model considering SSI effects. It is worth nothing that the structural model considering SSI effects tends to yield higher damage index compared with the fixed-base model, and the DPDMs behave different distribution compared with the MIDR.

Various uncertainties are taken into account through the log-standard deviation parameter β, which describes the total dispersion related to each fragility curve. Three primary sources of uncertainty contribute to the total variability for any given damage state [30], including the variability associated with structural modeling, the capacity of each structural type, and the seismic demand. The log-standard deviation value in the definition of limit states is assumed to be equal to 0.2 [31], while the corresponding value in the capacity is assumed to be 0.2, 0.3, and 0.4 for slight/moderate and severe/complete damage states, which considers that the uncertainty of the structural capacity increases with the deepening of structural damage [32]. The third source of uncertainty associated with the seismic demand is taken into consideration by calculating the dispersion of the logarithms of simulated results with respect to the regression fit. Under the assumption that these three log-standard deviation components are statistically independent, and the total log-standard deviation is estimated as the root of the sum of the squares of the component dispersions. The computed log-standard deviation β values of the fragility curves in terms of PGA-MIDR vary from 0.79 to 0.86 and 0.85 to 0.92 for the model considering SSI effects and the fixed-base model, respectively. However the β values for the DPDMs vary from 0.76 to 0.99 and from 0.73 to 1.07 for the model considering SSI effects and the fixed-base model, respectively.

Table 6 presents the lognormal distributed fragility parameters of median and log-standard deviation for the fixed-base building, and Figure 10 gives the comparative fragility

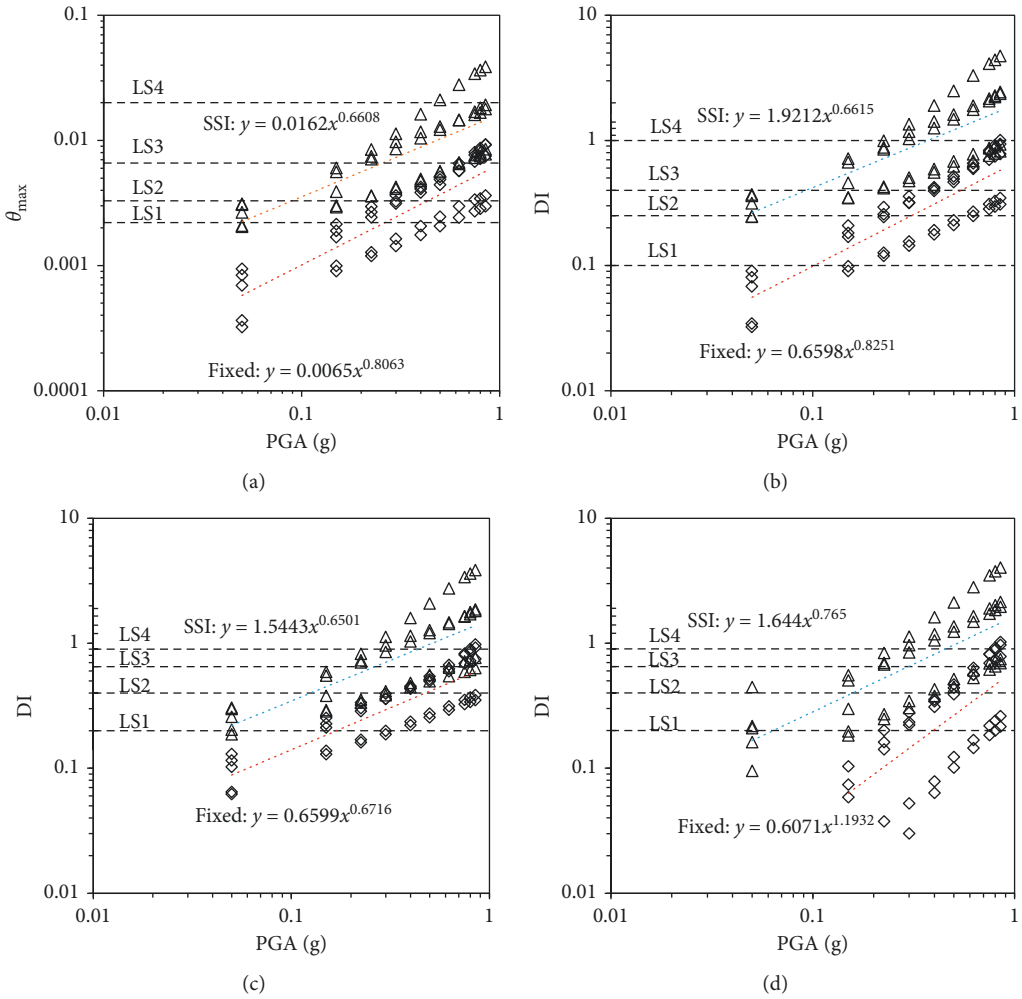

Figure 9: Comparative relationships for the SSI models based on (a) MIDR model and three double-parameter damage models: (b) Park–Ang model, (c) Niu model, and (d) Lu–Wang model.

Table 6: Parameters of the fragility functions in terms of PGA for the analysed structure without considering SSI effect.

Damage model	Median PGA (g)				Dispersion β			
	LS1	LS2	LS3	LS4	LS1	LS2	LS3	LS4
IMDR	0.29	0.46	1.03	3.69	0.85	0.88	0.88	0.92
Park–Ang	0.11	0.31	0.55	1.65	0.87	0.90	0.90	0.94
Niu	0.17	0.48	0.98	1.58	0.73	0.76	0.76	0.81
Lu–Wang	0.4	0.71	1.04	1.36	1.01	1.04	1.04	1.07

curves for different DPDMs of Park–Ang, Niu, and Lu–Wang compared with that of the MIDR damage index. It is shown that the fragility distribution of the fixed-base building is changed when DPDMs are adopted. From the slight damage state to the severe damage state, a significant overall increase of the fixed-base building's fragility of Park–Ang damage model with respect to the MIDR damage index. Especially in the complete damage state, the median values of Park–Ang, Niu, and Lu–Wang are far smaller than that of the MIDR. It shows the fragility of the fixed-base building is greatly reduced by adopting the MIDR compared with the DPDMs of Park–Ang, Niu, and Lu–Wang. It may be due to that the failure of the structure is mainly determined by the accumulated damage in this state, but the MIDR only takes the deformation into account. Thus, there is a big difference to evaluate the structural fragility using the DPDMs and the MIDR damage index, and therefore, it is unreasonable to only adopt the IMDR as the damage index for fragility analysis.

Table 7 summarizes the lognormal distributed fragility parameters (median and log-standard deviation) in terms of PGA-MIDR for the buildings with or without SSI effect. Figure 11 depicts the comparative fragility curves for the SSI and the fixed-base models using the MIDR damage index. From Figure 11, it can be seen that the SSI effects decrease the median values compared with those of the fixed-base model, which lead to that the SSI model presents higher fragility compared with that of the fixed-base models. This observation is noticeable for four limit damage limit states. The overall fragility of SSI models increased significantly even by 50%. It is indicated that the seismic performance of the structure is overestimated without considering SSI effects. But for the slight and the

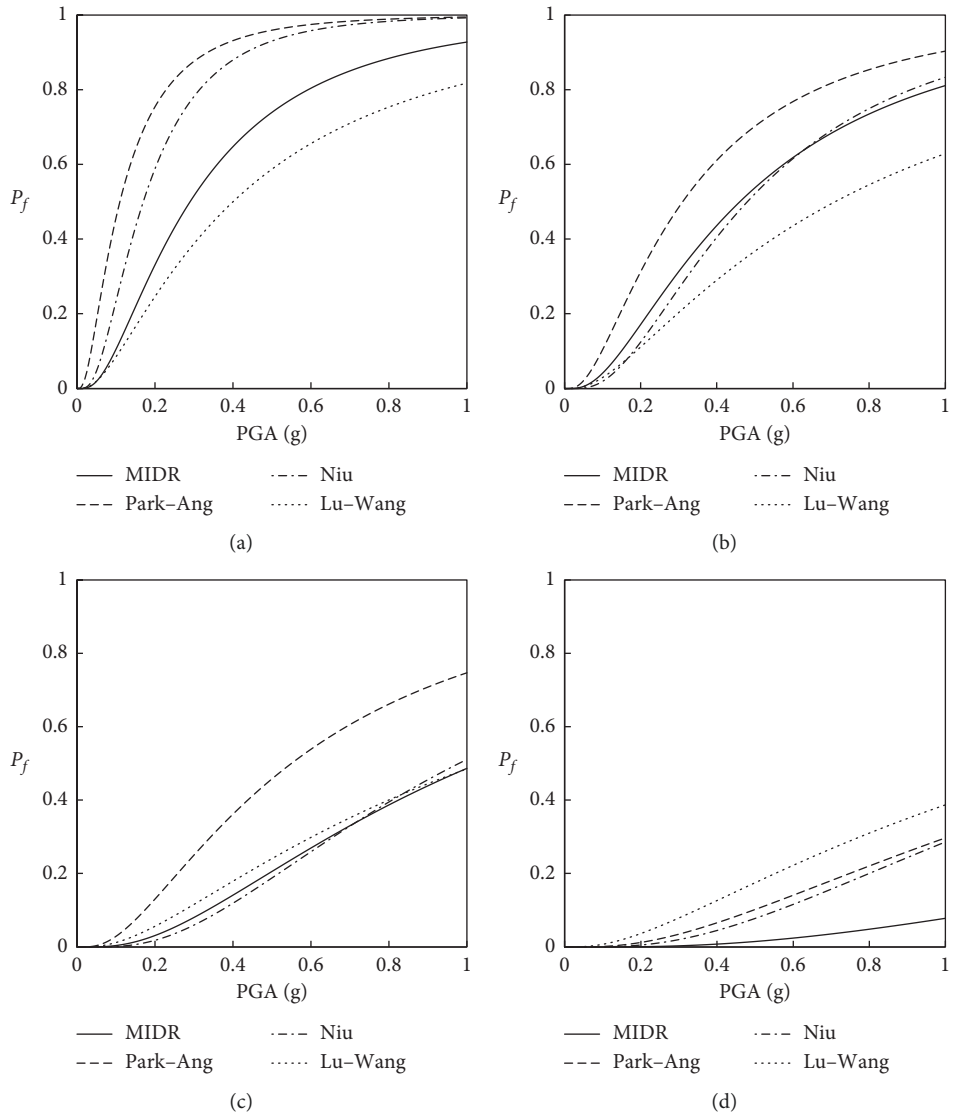

Figure 10: Fragility curves of the fixed-base building based on DPDMs compared with the MIDR damage index: (a) slight damage, (b) moderate damage, (c) severe damage, and (d) complete damage.

Table 7: Parameters of the fragility functions in terms of PGA-MIDR for the analysed structure with and without SSI effect.

RC buildings	Median PGA (g)				Dispersion β			
	LS1	LS2	LS3	LS4	LS1	LS2	LS3	LS4
Fixed base	0.29	0.46	1.03	3.69	0.85	0.88	0.88	0.92
SSI model	0.05	0.09	0.26	1.38	0.79	0.82	0.82	0.86

moderate damage states, the effects decrease the gap between the fragility of SSI model and that of the fixed-base model with the increase of PGA. Thus, SSI effects may play a crucial role in the expected structural damage, even if it is expressed in terms of the MIDR, and SSI effects should not be neglected for assessment purposes. The results here are similar to those in the study of Karapetrou et al. [33], which shows that considering the SSI effects leads to a significant increase in the fragility compared with that of the fixed base. Additionally, in the research of Rajeeva et al. [6], the reference structures are of three different heights, and all the fragility curves of the SSI models induce a higher fragility. The higher fragility could be because the SSI effect introduces additional translation and rotation effects and increases the displacement demands on the structure or resonance effect appears.

The obtained results show that the seismic behaviour of the structure will be affected when the SSI is considered, especially when using MIDR as the damage index, which will lead to an unsafe structure. Therefore, the SSI effects should not be neglected in the structural fragility analysis.

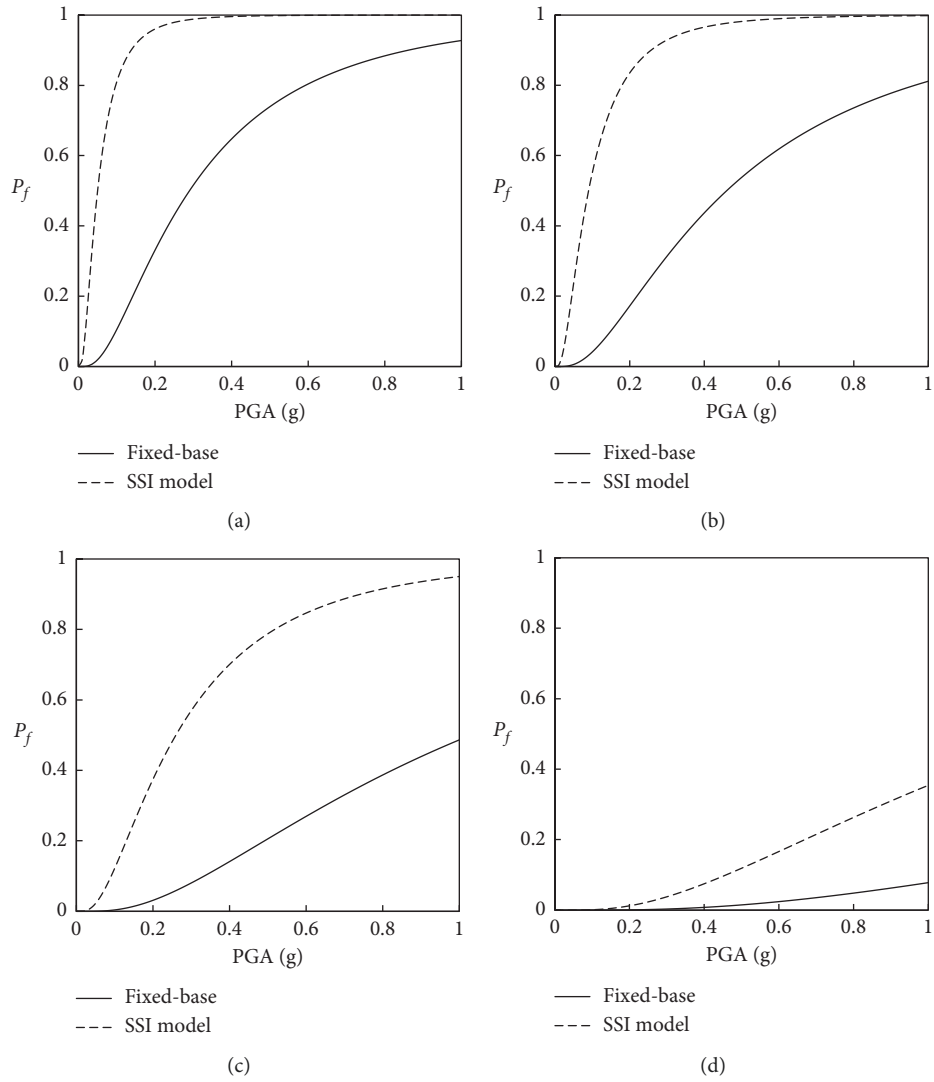

Figure 11: Comparative fragility curves between the double-parameter and single-parameter damage models: (a) slight damage, (b) moderate damage, (c) severe damage, and (d) complete damage.

Based on the analysis mentioned above, it can be seen that SSI effect has a great impact on the fragility of the structure using the MIDR as the damage index. But the MIDR only considers the structural damage caused by deformation, which could underestimate the damage degree, especially under a long-lasting earthquake. However, the DPDMs taking the combination of the deformation and energy as the damage index can reflect both the maximum deformation and cumulative damage effects, which is thought to be more comprehensive at describing the structural damage.

Table 8 summarizes the lognormal distributed fragility parameters including the median and log-standard deviation in terms of PGA for the building considering SSI effects with three DPDMs and the MIDR. Figure 12 depicts the comparative fragility curves for three different DPDMs of PA model, Niu model, and Lu–Wang model compared with that of the MIDR. It is shown that adopting the double-parameter damage index behaves different fragility distribution compared with the single-parameter index of MIDR. From the slight damage state to the severe damage state, it can be seen that the median value of MIDR is higher that of PA model and Niu model but is lower than that of Lu–Wang model. So the fragility of PA and Niu models is higher than that of MIDR, and the fragility of Lu–Wang model is the lowest. For the complete damage state, the median values of the three DPDMs are all far lower than that of MIDR, which leads to the failure probability of the structure in this state that is much smaller than that of the double-parameter damage index. This may be attributed to that the proportion of the cumulative damage on the structural damage is increased, and the cumulative damage gradually dominates the structural damage in this state, while the MIDR does not consider this part, so the fragility of MIDR is far lower than that of DPDMs.

Next, regarding the influence of the SSI effects on the fragility of DPDMs compared with the fixed-base building, comparing the median values of Tables 6 and 8, as well as

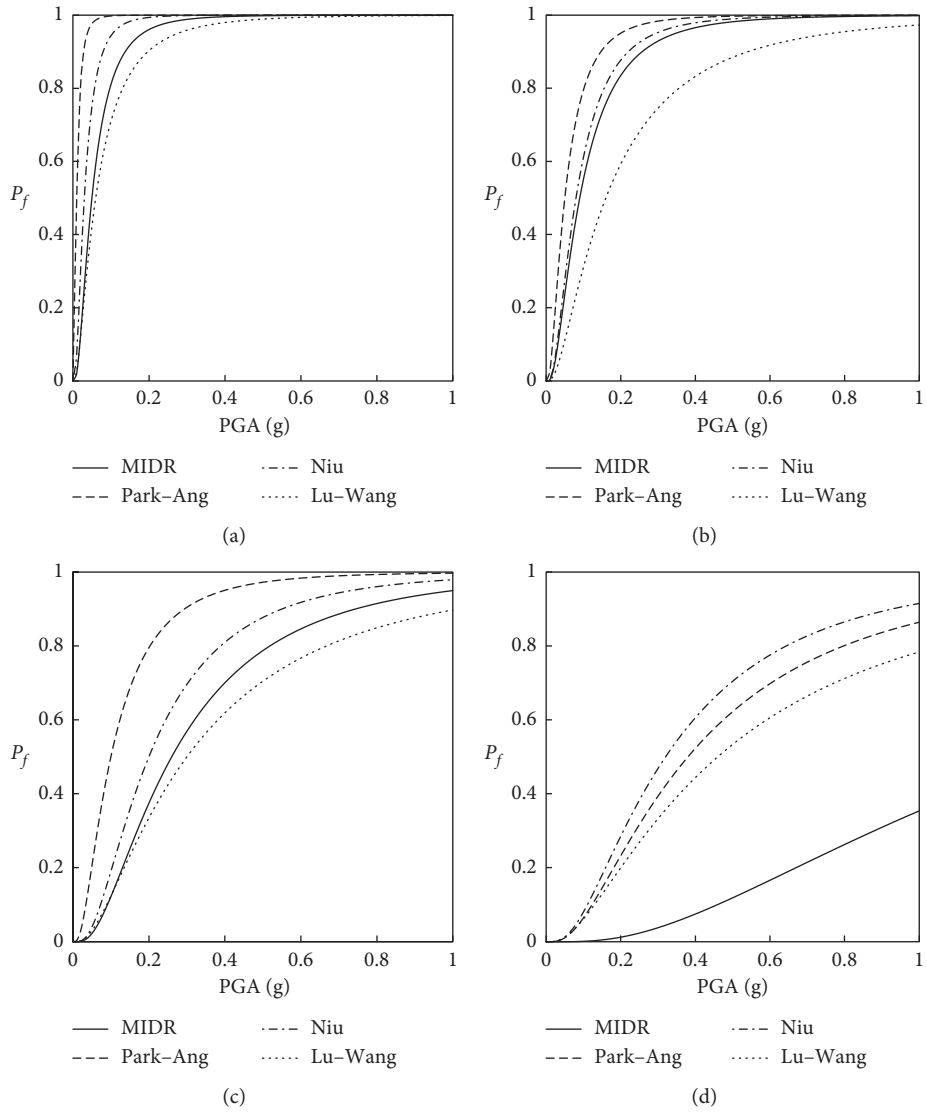

Figure 12: Fragility curves of the fixed-base and SSI models with MIDR:(a) slight damage, (b) moderate damage, (c) severe damage, and (d) complete damage.

Table 8: Parameters of the fragility functions in terms of PGA for the analysed structural models with considering SSI by adopting IMDR and DPDMs.

Damage model	Median PGA (g)				Dispersion β			
	LS1	LS2	LS3	LS4	LS1	LS2	LS3	LS4
MIDR	0.05	0.09	0.26	1.38	0.79	0.82	0.82	0.86
Park–Ang	0.01	0.05	0.1	0.38	0.81	0.84	0.84	0.88
Niu	0.03	0.08	0.2	0.32	0.76	0.79	0.79	0.83
Lu–Wang	0.06	0.16	0.3	0.46	0.93	0.95	0.95	0.99

the fragility curves of Figures 10 and 12, it is seen that SSI effects also increase the fragility of the buildings compared with the fixed-base case using DPDMs. Especially for the severe and complete damage states, this observation is more noticeable.

Therefore, it is more reasonable and comprehensive to employ the DPDMs to describe and evaluate the seismic fragility of the SSI model, while adopting the MIDR will lead to an underestimate of the seismic fragility of the structure and will cause the structure to be unsafe, especially in the complete damage state.

6. Conclusions

There are two objectives presented in this study. One is to investigate the SSI effects on the structural fragility

compared with those of the fixed-base model. The results represented in this study show that consideration of the SSI effects induces a higher fragility than that of the fixed-base model by adopting both the DPDMs and the IMDR, and it will lead to the structure being unsafe. Therefore, the SSI effects should not be neglected in the structural fragility analysis.

The other objective is to supply a method for fragility assessment to study the influence of the DPDMs on the SSI structural fragility analysis compared with the MIDR. First, a series of dynamic analyses are conducted based on three DPDMs compared with the MIDR for the building with and without considering SSI effects. It shows that the building using the MIDR will lead to a significant decrease in the damage assessment compared with the DPDMs of Park–Ang, Niu, and Lu–Wang models. With the increase in PGA, the difference in damage assessment using the DPDMs is more noticeable than that assessed using the MIDR. Next, IDA is performed by 50 scaled input ground motions, and the fragility curves based on the DPDMs are obtained compared with that of the MIDR. It is shown that adopting the DPDMs of Park–Ang, and Niu increases the fragility compared with that of the MIDR from the slight damage state to the severe damage state, but the Lu–Wang damage model decreases the fragility of the structure in the corresponding damage state. More significantly, in the complete damage state, the MIDR greatly increases the fragility of the structure compared with that of Park–Ang, Niu, and Lu–Wang damage models, which will overestimate the structural seismic capacity to lead to severe seismic losses. Therefore, it is more reasonable to adopt the DPDMs for fragility analysis by considering SSI effects.

All these conclusions are based on the results of the eight-story RC building supported by pile foundation on soft soil. Other influential factors (e.g., number of stories, structural types, foundation types, and soil types) will be considered in future studies.

Data Availability

The data used to support the findings of this study are included within the article.

Conflicts of Interest

The authors declare that they have no conflicts of interest.

Acknowledgments

This work was partially developed in the framework of the research project funded by the Sichuan International Science and Technology Innovation Cooperation/Hong Kong, Macao and Taiwan Science and Technology Innovation Cooperation (2019YFH0120).

References

[1] G. M. Calvi, R. Pinho, G. Magenes et al., "Development of seismic vulnerability assessment methodologies over the past 30 years," *ISET Journal of Earthquake Technology*, vol. 43, no. 3, pp. 104–175, 2006.

[2] M. Shinozuka, M. Q. Feng, J. Lee, and T. Naganuma, "Statistical analysis of fragility curves," *Journal of Engineering Mechanics*, vol. 126, no. 12, pp. 1224–1231, 2000.

[3] K. Z. W. Myat, *Analysis on Seismic Performance of Strip Foundation of a Low Rise Building with Soil-Structure Interaction Approach*, 2008.

[4] S. C. Dutta, K. Bhattacharya, and R. Roy, "Response of low-rise buildings under seismic ground excitation incorporating soil-structure interaction," *Soil Dynamics and Earthquake Engineering*, vol. 24, no. 12, pp. 893–914, 2004.

[5] P. E. Pinto and M. Ciampoli, "Effects of soil-structure interaction on inelastic seismic response of bridge piers," *Journal of Structural Engineering*, vol. 121, no. 5, pp. 806–814, 1995.

[6] P. Rajeev and S. Tesfamariam, "Seismic fragilities of non-ductile reinforced concrete frames with consideration of soil structure interaction," *Soil Dynamics and Earthquake Engineering*, vol. 40, no. 3, pp. 78–86, 2012.

[7] K. D. Pitilakis, S. T. Karapetrou, and S. D. Fotopoulou, "Consideration of aging and SSI effects on seismic vulnerability assessment of RC buildings," *Bulletin of Earthquake Engineering*, vol. 12, no. 4, pp. 1755–1776, 2014.

[8] E. Sáez, F. Lopez-Caballero, and A. Modaressi-Farahmand-Razavi, "Effect of the inelastic dynamic soil-structure interaction on the seismic vulnerability assessment," *Structural Safety*, vol. 33, no. 1, pp. 51–63, 2011.

[9] M. E. Rodriguez and J. C. Aristizabal, "Evaluation of a seismic damage parameter," *Earthquake Engineering & Structural Dynamics*, vol. 28, no. 5, pp. 463–477, 2015.

[10] Y. J. Park and A. H. S. Ang, "Mechanistic seismic damage model for reinforced concrete," *Journal of Structural Engineering*, vol. 111, no. 4, pp. 722–739, 1985.

[11] Y. J. Park, A. M. Reinhorn, and S. K. Kunnath, "IDARC: inelastic damage analysis of reinforced concrete frame-shear wall structures," Technical Report, National Center for Earthquake Engineering Research, Taipei, Taiwan, 1987.

[12] D. Niu and L. Ren, "A modified seismic damage model with double variables for reinforced concrete structures," *Earthquake Engineering and Engineering Vibration*, vol. 16, no. 4, pp. 45–55, 1996, in Chinese.

[13] D. Lu and W. Guangyuan, "Decision making method for optimal design of earthquake resistant structures based on damage performance," *Civil Engineering Journal*, vol. 34, no. 1, pp. 44–49, 2001, in Chinese.

[14] D. Lu, "Intelligent optimization design of disaster resistant structures based on optimal fortification load and performance," Doctoral Dissertation, Harbin University of Architecture, Heilongjiang, China, 1999.

[15] X. Du and J. Ou, "Seismic damage assessment model of buildings," *World Earthquake Engineering*, vol. 7, no. 3, pp. 52–58, 1991, in Chinese.

[16] J. Ou, Z. He, B. Wu, and L. Xu, "Seismic damage control design of reinforced concrete structures," *Journal of Buildings Structures*, vol. 21, no. 1, pp. 63–67, 2000, in Chinese.

[17] J. M. Bracci, A. M. Reinhorn, J. B. Mander et al., "Deterministic model for seismic damage evaluation of reinforced concrete structures," Technical Report, State University, New York, NY, USA, 1989.

[18] Y. Li, B. Liu, and Q. Shi, "Performance levels and estimation indices of structures," *World Earthquake Engineering*, vol. 19, no. 2, pp. 132–137, 2003, in Chinese.

[19] National Standard of the People's Republic of China (NSPRC), *Code for Seismic Design of Buildings (GB50011-2010)*, Ministry of Construction of Peoples Republic of China, Beijing, China, 2010.
[20] National Standard of the People's Republic of China (NSPRC), *Code for Concrete Structure Design (GB 50010-2010)*, Ministry of Construction of Peoples Republic of China, Beijing, China, 2010.
[21] D., Kong, *Study on Equivalent Method of Reinforced Concrete Material Properties*, Shenyang Jianzhu University, Shenyang, China, 2003.
[22] Y. H. Zhao and G. J. Weng, "Effective elastic moduli of Ribbon-reinforced Composites," *Journal of Applied Mechanics*, vol. 57, no. 1, pp. 158–167, 1990.
[23] Y. H. Zhao, G. P. Tandon, and G. J. Weng, "Elastic moduli for a class of porous materials," *Acta Mechanica*, vol. 76, no. 1-2, pp. 105–131, 1989.
[24] Z. Pan, *Research and Application of Reinforced Concrete Equivalent Material*, Harbin Institute of Technology, Heilongjiang, China, 2008.
[25] Z. Lu and B. Jiang, "Study on range of mesh about finite element for back analysis of displacement," *China Civil Engineering Journal*, vol. 32, no. 1, pp. 26–30, 1999, in Chinese.
[26] D. C. Drucker, W. Prager, and H. J. Greenberg, "Extended limit design theorems for continuous media," *Quarterly of Applied Mathematics*, vol. 9, no. 4, pp. 381–389, 1952.
[27] D. C. Drucker and W. Prager, "Soil mechanics and plastic analysis or limit design," *Quarterly of Applied Mathematics*, vol. 10, no. 2, pp. 157–165, 2013.
[28] D. Vamvatsikos and C. A. Cornell, "Incremental dynamic analysis," *Earthquake Engineering and Structural Dynamics*, vol. 31, no. 3, pp. 491–514, 2002.
[29] Y. K. Wen, B. R. Ellingwood, and J. M. Bracci, "Vulnerability function framework for consequence-based engineering," Technical Report No.DS-4, Mid-America Earthquake Center (MAE), University of Illinois at Urbana-Champaign, Champaign, IL, USA, 2004.
[30] National Institute of Building Science, *Direct Physical Damage-General Building Stock, HAZUS-MH Technical Manual, Chapter 5*, Federal Emergency Management Agency, Washington, DC, USA, 2004.
[31] B. R. Ellingwood, O. C. Celik, and K. Kinali, "Fragility assessment of building structural systems in Mid-America," *Earthquake Engineering and Structural Dynamics*, vol. 36, no. 13, pp. 1935–1952, 2007.
[32] X. Yu, D. Lu, and B. Li, "Estimating uncertainty in limit state capacities for reinforced concrete frame structures through pushover analysis," *Earthquakes and Structures*, vol. 10, no. 1, pp. 141–161, 2016.
[33] S. T. Karapetrou, S. D. Fotopoulou, and K. D. Pitilakis, "Seismic vulnerability assessment of high-rise non-ductile RC buildings considering soil-structure interaction effects," *Soil Dynamics and Earthquake Engineering*, vol. 73, pp. 42–57, 2015.